Monatshefte für Chemie 115, 997—1012 (1984)

Monatshefte für Chemie
Chemical Monthly

Physical Adsorption of Gases on Energetically Heterogeneous Solids I. Generalized *Langmuir* Equation and Its Energy Distribution

Mieczysław Jaroniec and **Adam W. Marczewski**

Institute of Chémistry, M. Curie-Skłodowska University, PL-20031 Lublin, Poland

(Received 21 February 1984. Accepted 19 March 1984)

A generalized *Langmuir* equation is proposed for describing the monolayer adsorption of single gases on heterogeneous solids. The special cases of this equation are: *Langmuir-Freundlich, Tóth* and *Freundlich* type adsorption isotherms. The energy distribution function corresponding to this equation produces all types of simple energy distributions, i.e., symmetrical distribution, decreasing exponential distributions and asymmetrical distributions showing widening in the directions of low and high adsorption energies.

(Keywords: Gas adsorption; Heterogeneous solids)

Gasadsorption auf energetisch heterogenen Feststoffen, 1. Mitt.: Eine generalisierte Langmuir-Gleichung und ihre Energieverteilung

Es wird eine generalisierte *Langmuir*-Gleichung zur Beschreibung der einlagigen Adsorption eines einzelnen Gases auf heterogenen Feststoffen beschrieben. Die speziellen Fälle dieser Gleichung sind: *Langmuir-Freundlich-*, *Tóth-* und *Freundlich*-Typ der Adsorptionsisotherme. Die Energieverteilung, die dieser Gleichung entspricht, gibt alle Typen einer einfachen Verteilung wieder, z. B. eine symmetrische Verteilung, eine abfallende exponentielle Verteilung und asymmetrische Verteilungen mit Erweiterung in die Richtung von niedriger oder hoher Adsorptionsenergie.

Introduction

The majority of isotherm equations for gas adsorption on heterogeneous solid surfaces has been derived by solving the integral equation:

$$\theta_t(p) = \int_{\Delta} \theta_l(p, \varepsilon) F(\varepsilon) \, d\varepsilon \tag{1}$$

for the *Langmuir* local isotherm $\theta_l(p, \varepsilon)$:

$$\theta_l(p, \varepsilon) = [1 + (K_0 \cdot p)^{-1} \exp(-\varepsilon/RT)]^{-1} \tag{2}$$

and different energy distributions $F(\varepsilon)$[1—6].

In the above equations $\theta_l(p)$ is the overall adsorption isotherm, p is the adsorptive pressure, ε is the adsorption energy, K_0 is the pre-exponential factor of the *Langmuir* constant and Δ is the integration region for ε. These equations may be divided into two groups[7]. The equations belonging to the first group contain one additional parameter in comparison to the *Langmuir* isotherm and they become the *Langmuir* equation when this parameter is equal to unity. However, the equations belonging to the second group may be treated as special cases of the exponential adsorption isotherm proposed in 1975 by *Jaroniec*[6]. They are: the classical *Freundlich* isotherm, the *Dubinin-Radushkevich* and *Dubinin-Astakhov* equations[7]. Nevertheless, these equations differ strongly from the *Langmuir* isotherm and their derivation by integrating Eq. (1) for the *Langmuir* Eq. (2) and definite energy distributions are approximate[3]. This means that equations of the second group, although playing an important role in physical adsorption, are still insufficiently explained[8—10]. As opposed to these equations the adsorption isotherms belonging to the first group may be exactly obtained by integrating Eq. (1) for the *Langmuir* Eq. (2) and definite energy distributions.

In this paper a new isotherm equation is proposed for gas adsorption on heterogeneous solid surfaces. It is analogous to an equation used recently by *Marczewski* and *Jaroniec*[11] for describing single-solute adsorption from dilute solutions on solids. All equations belonging to the first group mentioned above are special cases of this equation. The new adsorption isotherm contains four parameters, which may be evaluated by simple independent methods from experimental adsorption isotherms. The mathematical and physical properties of this isotherm equation are widely discussed. For the purpose of illustration, this equation is applied to evaluate the adsorption parameters and energy distribution function for model and experimental adsorption isotherms.

Results and Discussion

General Considerations

The local surface coverage θ_l, predicted by the *Langmuir* isotherm Eq. (2), is equal to zero for $p = 0$ and tends to unity when the pressure tends to infinity. Since the energy distribution $F(\varepsilon)$ is normalized to unity, i.e.:

$$\int_{\Delta} F(\varepsilon)\, d\varepsilon = 1 \tag{3}$$

the overall surface coverage θ_t, represented by the integral Eq. (1), should show the same limiting values as the *Langmuir* Eq. (2). This means that the overall isotherm equations generated by the *Langmuir* local isotherm should be equal to zero at $p = 0$ and reach unity at infinite pressure. Such mathematical properties show the overall isotherm equations belonging to the first group, i.e., the generalized *Freundlich* (GF)[2,3], the *Langmuir-Freundlich* (LF)[1] and the *Tóth* (T) isotherm[5]. However, the overall isotherms belonging to the second group are equal to unity at a finite value of pressure[6]. Therefore, *Misra*[4] modified the classical *DR* isotherm and his equation tends to unity when pressure tends to infinity. Although this modified isotherm shows identical behaviour at limiting values of pressure as the *Langmuir* Eq. (2), some of its mathematical properties are different from those referring to the adsorption isotherms for the first group. Moreover, the overall adsorption isotherms obtained by means of Eqs. (1) and (2) satisfy the following inequalities:

$$0 < \varphi_t(p) < 1 \quad \text{for} \quad p \in (0, \infty) \tag{4}$$

and

$$-1 < \varphi_t^*(p) < 0 \quad \text{for} \quad p \in (0, \infty) \tag{5}$$

where

$$\varphi_t(p) = \frac{\partial \ln \theta_t}{\partial \ln p} \tag{6}$$

$$\varphi_t^*(p) = \frac{\partial \ln (1 - \theta_t)}{\partial \ln p} \tag{7}$$

Analogous inequalities are also fulfilled for the *Langmuir* Eq. (2):

$$0 < \varphi_l(p) < 1 \quad \text{for} \quad p \in (0, \infty) \tag{8}$$

and

$$-1 < \varphi_l^*(p) < 0 \quad \text{for} \quad p \in (0, \infty) \tag{9}$$

where

$$\varphi_l(p) = \frac{\partial \ln \theta_l}{\partial \ln p} = 1 - \theta_l \tag{10}$$

$$\varphi_l^*(p) = \frac{\partial \ln (1 - \theta_l)}{\partial \ln p} = -\theta_l \tag{11}$$

The mathematical properties of the functions $\varphi_t(p)$, $\varphi_t^*(p)$, $\varphi_l(p)$, $\varphi_l^*(p)$ at limiting values of pressure are summarized in Table 1.

Table 1. *Limiting values of the functions defined by Eqs. (6), (7), (10), and (11)*

Function φ	Value of φ at $p = 0$	Value of φ at $p \to \infty$
$\varphi_t(p)$	$\leqslant 1$	$= 0$
$\varphi_l(p)$	$= 1$	$= 0$
$\varphi_t^*(p)$	$= 0$	$\geqslant -1$
$\varphi_l^*(p)$	$= 0$	$= -1$

A New Adsorption Isotherm

Let us define the following function:

$$\psi_1 = \ln\left[\frac{\partial \ln p}{\partial \ln a} - 1\right] \tag{12}$$

where a is the adsorbed amount at a given value of pressure. For the *Langmuir* Eq. (2) this function becomes:

$$\psi_1^L = \ln K + \ln p \tag{13}$$

where

$$K = K_0 \cdot \exp(\varepsilon/RT) \tag{14}$$

The dependence of ψ_1 on $\ln p$ is linear, the slope is equal to unity. *Tóth*[12,13] showed that Eq. (13), being just another form of the *Langmuir* Eq. (2), has a strong limitation on its application, because only a few adsorption systems follow this relationship. Therefore, *Tóth*[12,13] improved the *Langmuir* Eq. (2). His new adsorption isotherm gives the following relationship for ψ_1:

$$\psi_1 = n \cdot \ln \bar{K} + n \cdot \ln p \tag{15}$$

where $\bar{K}$ is a constant analogous to the *Langmuir* constant K (this will be explained later) and n is a parameter varying from zero to unity. For $n = 1$ Eq. (15) becomes Eq. (13).

Our studies show that Eq. (15) fulfils considerably better experimental adsorption data than Eq. (13), although in many cases its agreement with experiment is not satisfactory. To improve Eq. (15) we

propose a small modification of this equation. According to this modification the function:

$$\psi_m = \ln\left[m\left(\frac{\partial \ln p}{\partial \ln a}\right) - 1\right] \tag{16}$$

fulfils the right side of Eq. (15); m is the heterogeneity parameter analogous to n and varying from zero to unity.

The physical meaning of m and n will be explained in the next section. After our modification Eq. (15) assumes the following form:

$$\psi_m = n \cdot \ln \bar{K} + n \cdot \ln p \tag{17}$$

Eq. (17) gives:

$$\frac{\partial \ln a}{\partial \ln p} = \frac{m}{1 + (\bar{K}p)^n} \tag{18}$$

However, *Tóth*[12] considered the following relationship:

$$\frac{\partial \ln a}{\partial \ln p} = \frac{1}{1 + (\bar{K}p)^n} \tag{19}$$

which is a special case of Eq. (18) for $m = 1$.

Integrating Eq. (18) with respect to p and taking into account the limiting condition:

$$\lim_{p \to \infty} a(p) = a_0 \tag{20}$$

we obtain:

$$\theta_t(p) = \left[\frac{(\bar{K}p)^n}{1 + (\bar{K}p)^n}\right]^{m/n} \tag{21}$$

where

$$\theta_t(p) = a/a_0 \tag{22}$$

Eq. (21) comprises all isotherm equations belonging to the first group (cf., Table 2) and may be treated as a more general form of the overall adsorption isotherm generated by the *Langmuir* equation (generalized *Langmuir* equation—G*L*E).

In the review[7] *Jaroniec* considered also the *Radke-Prausnitz* equation (*RP*E):

$$1/\theta_t = 1/\bar{K}p + 1/Ap^r \tag{23}$$

as an extension of the *Langmuir* Eq. (2). In this equation A is the parameter connected with the constant $\bar{K}$ and r is the parameter varying from zero to unity. This equation may be also obtained also from GLE Eq. (21). Developing the denominator of Eq. (21) into *Taylor*'s series with respect to (p^n) about the point $p^n = 0$, we have:

$$[1 + (\bar{K}p)^n]^{m/n} = 1 + \frac{m}{n}(\bar{K}p)^n + \ldots \tag{24}$$

Table 2. *Special cases of* GLE *expressed by Eq. (21)*

m	n	Isotherm equation	Abbreviations[a]
1	1	$\theta = Kp/(1 + Kp)$	*LE* (*Langmuir* Eq.)
(0,1)	1	$\theta_t = [\bar{K}p/(1 + \bar{K}p)]^m$	*GFE* (generalized *Freundlich* Eq.)
1	(0,1)	$\theta_t = \bar{K}p/[1 + (\bar{K}p)^n]^{1/n}$	*TE* (*Tóth* Eq.)
(0,1)	$n = m$	$\theta_t = (\bar{K}p)^m/[1 + (\bar{K}p)^m]$	*LFE* (*Langmuir-Freundlich* Eq.)

[a] Abbreviations of the adsorption isotherm designations summarized in this table are taken from the references[2, 3, 5, 7, 14].

Neglecting higher terms and combining it with Eq. (21) we obtain the following relationship:

$$\frac{1}{\theta_t} = \frac{1}{(\bar{K}p)^m} + \frac{1}{\frac{n}{m}(\bar{K}p)^{m-n}} \tag{25}$$

which for $m = 1$ gives:

$$\frac{1}{\theta_t} = \frac{1}{\bar{K}p} + \frac{1}{n(\bar{K}p)^{1-n}} \tag{26}$$

Eq. (26) is identical with the *RP* Eq. (23), where $A = n\bar{K}^{1-n}$ and $r = 1 - n$. As *RP* Eq. (23) has been obtained for low pressures, it shows improper behaviour for pressures tending to infinity; at $p \to \infty$ the surface coverage tends to infinity. However, this equation and the *Tóth* isotherm predict *Henry*'s law at low pressures, whereas in this pressure region the *GF* and *LF* isotherms become the classical *Freundlich* equation:

$$\theta_t = (\bar{K}p)^m \tag{27}$$

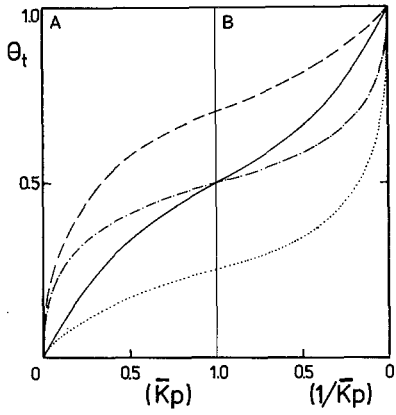

Fig. 1. Theoretical adsorption isotherms calculated according to Eq. (21) for $m = n = 1$ (LE) (the solid line), $m = n = 0.5$ (LFE) (the dashed-dotted line), $m = 1$ and $n = 0.5$ (TE) (the dotted line), $m = 0.5$ and $n = 1.0$ (GFE) (the dashed line)

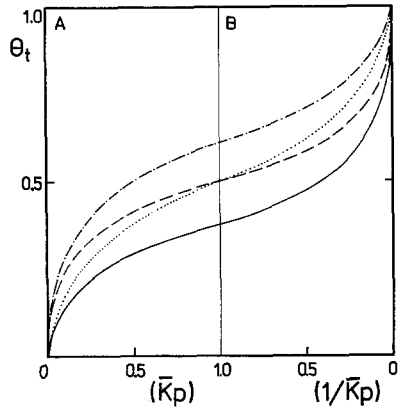

Fig. 2. Theoretical adsorption isotherms calculated according to Eq. (21) for $m = n = 0.5$ (LFE) (the dashed line), $m = n = 0.7$ (LFE) (the dotted line), $m = 0.5$ and $n = 0.7$ (the dashed-dotted line), $m = 0.7$ and $n = 0.5$ (the solid line)

The above difference between adsorption isotherms belonging to the first group may be explained by means of the energy distributions corresponding to them. This problem is discussed in the Appendix.

The mathematical properties of the GL Eq. (21) and its special cases are presented in Figs. 1 and 2. These figures show the theoretical

adsorption isotherms calculated according to Eq. (21) for different values of m and n. The surface coverage θ_t is plotted as a function of $(\bar{K}p)$ for $(\bar{K}p)$ varying from zero to unity and as a function of $(1/\bar{K}p)$ for $(\bar{K}p)$ varying from unity to infinity. The isotherm curves presented in Figs. 1 and 2 are continuous increasing functions because they are plotted for increasing $(\bar{K}p)$ in the region (0, 1) and decreasing $(\bar{K}p)^{-1}$ in the region (1, 0); in such combined axis the pressure is still increasing and at the point $(\bar{K}p) = (\bar{K}p)^{-1} = 1$ two parts of an adsorption isotherm unite. The above presentation of adsorption isotherms is better than the traditional one, i.e., θ_t vs. $(\bar{K}p)$ in the whole pressure range, because it shows expressively differences between isotherm curves in the region of high pressures (also for experimental isotherms—in this case we can treat the approximate value of $\bar{K}_{appr}$ as an exact one—obtaining also the continuous increasing functions).

Fig. 1 shows the isotherm curves calculated according to Eq. (21) for $m = n = 1$ (LE), $m = n = 0.5$ (LFE), $m = 1$ and $n = 0.5$ (TE), $m = 0.5$ and $n = 1$ (GFE). It follows from this figure that the curves refering to LE and LFE show a similar behaviour and lie between the GF isotherm (the upper curve) and *Tóth* isotherm (the lower curve).

Fig. 2 presents the adsorption isotherms calculated according to Eq. (21) for $m = n = 0.5$ (the dashed line), $m = n = 0.7$ (the dotted line), $m = 0.5$ and $n = 0.7$ (the dashed-dotted line), $m = 0.7$ and $n = 0.5$ (the solid line). The isotherm curves plotted for $m = n$ (LF isotherms) intersect at $\theta_t = 0.5$ and $\bar{K}p = 1$. In the range of $\bar{K}p$ varying from zero to unity a decrease in m causes an increase in θ_t.

An opposite behaviour of the overall isotherm is observed for LFE and $(1/\bar{K}p)$ varying from unity to zero. For $m \neq n$ the adsorption isotherm curves are similar to GF isotherm when $m < n$ or *Tóth* isotherm when $m > n$.

Energy Distribution Corresponding to GLE

The energy distribution function corresponding to Eq. (21) may be calculated according to the *Stieltjes* transform method used by many authors[1–7]. This method gives:

$$F(\varepsilon) = \frac{\sin\left(\frac{m}{n}\gamma\right)}{\pi RT\,[\exp(2nE) + 2\cos(\pi n)\exp(nE) + 1]^{m/2n}} \tag{28}$$

where

$$\gamma = \arccos \frac{\cos(\pi n)\exp(nE) + 1}{[\exp(2nE) + 2\cos(\pi n)\exp(nE) + 1]^{1/2}} \tag{29}$$

and

$$E(\varepsilon) = E = (\varepsilon - \varepsilon_0)/RT \tag{30}$$

The heterogeneity parameters m and n characterize the width of the energy distribution, whereas the energy ε_0 determines the position of $F(\varepsilon)$ on the energy axis. The energy ε_0 is connected with the parameter $\bar{K}$ by a relationship analogous to Eq. (14):

$$\bar{K} = K_0 \exp(\varepsilon_0/RT) \tag{31}$$

For special values of m and n Eq. (28) gives the energy distributions corresponding to LFE, GFE and TE, which are summarized in Table 2. For $m = n$ Eq. (28) becomes:

$$F(\varepsilon) = \frac{\sin(\pi m)}{\pi RT[\exp(mE) + 2\cos(\pi m) + \exp(-mE)]} \tag{32}$$

The energy distribution corresponds to the LFE and for $E \to \pm\infty$ it is approximated by:

$$\ln[F(\varepsilon)] = \ln\left[\frac{\sin(\pi m)}{\pi RT}\right] \pm mE \tag{33}$$

However, the energy distribution corresponding to the TE [Eq. (21) with $m = 1$] is given by Eq. (28) with $m = 1$ and fulfils the following conditions:

$$\ln[F(\varepsilon)] = \ln\left[\frac{\sin(\pi n)}{n\pi RT}\right] - (n+1)\cdot E \quad \text{for} \quad E \to \infty \tag{34}$$

and

$$\ln[F(\varepsilon)] = \ln\left[\frac{m\sin(\pi n)}{n\pi RT}\right] + nE \quad \text{for} \quad E \to -\infty \tag{35}$$

The energy distribution relating to GFE [Eq. (21) with $n = 1$] may be also obtained from Eq. (28) replacing n by unity; it is:

$$F(\varepsilon) = \begin{cases} \dfrac{\sin(m\pi)}{\pi RT[\exp(E) - 1]^m} & \text{for } \varepsilon > \varepsilon_0 \\ 0 & \text{for } \varepsilon \leqslant \varepsilon_0 \end{cases} \tag{36}$$

For $E \to \infty$ Eq. (36) fulfils the same condition as the energy distribution corresponding to LFE, i.e., Eq. (33).

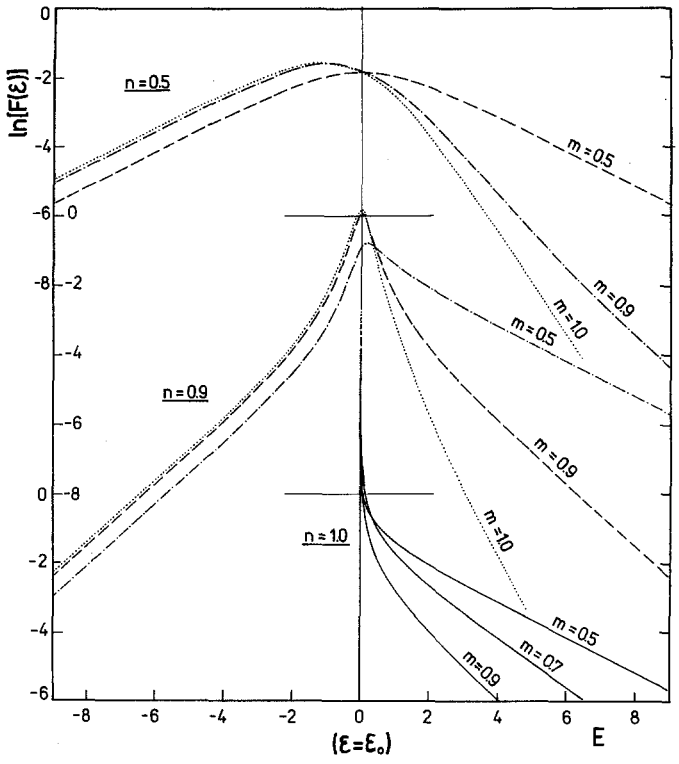

Fig. 3. Functions $\ln[F(\varepsilon)]$ calculated according to Eq. (28) for different values of m and fixed values of $n \in (0,1\rangle$. The solid lines refer to GF distributions, the dashed lines refer to LF distributions, the dotted lines refer to *Tóth* distributions and the dashed-dotted lines refer to GL distributions. The zero values of the function $\ln[F(\varepsilon)]$ are marked by horizontal thin solid lines

Figs. 3 and 4 show the functions $\ln[F(\varepsilon)]$ calculated according to Eq. (28) for different values of m and n. The functions $\ln[F(\varepsilon)]$ plotted for different values of m and a fixed value of $n \in (0, 1)$ are parallel at $E \to -\infty$ (cf., Fig. 3). The slope of the curves $\ln[F(\varepsilon)]$ plotted for different values of n and a fixed value of $m \in (0, 1)$ is identical at $E \to \infty$ and it is equal to minus m (cf., Fig. 4). Moreover, these functions coincide at $E \to \infty$. However, the curves $\ln[F(\varepsilon)]$ plotted for $n \in (0, 1)$ and $m = 1$ have slopes equal to $-(n + 1)$. The distribution functions calculated according to Eq. (28) for $m = n$ are symmetrical. However, the distributions calculated for $m \neq n$ are asymmetrical. If $m > n$ they are widened in the direction of $\varepsilon \to 0$, however, for $m < n$ they are widened in the direction of $\varepsilon \to \infty$. In the case of asymmetrical distributions a

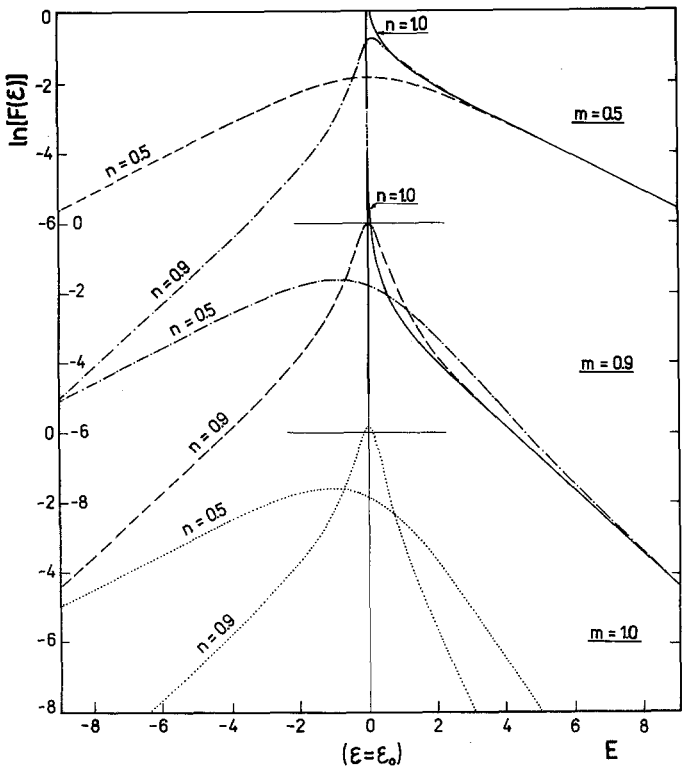

Fig. 4. Functions $\ln[F(\varepsilon)]$ calculated according to Eq. (28) for different values of n and fixed values of $m \in (0,1\rangle$; the labelling as in Fig. 3

decrease in the value of n causes mainly an extension of the function on the negative axis of E, however, a decrease in the value of m causes an extension of $F(\varepsilon)$ on the positive axis of E.

Relationships Obtained from GLE

For very low pressures the GLE (Eq. (21) reduces to the classical *Freundlich* Eq. (27), the linear form of which may be useful for determining the parameter m; it is:

$$\ln a = (m \ln \bar{K} + \ln a_0) + m \ln p \tag{37}$$

where a is the adsorbed amount and a_0 is the parameter defining the monolayer relative surface coverage $\theta_t = a/a_0$.

The parameter m may be also evaluated by means of the function $\varphi_t(p)$, which for Eq. (21) is expressed as follows:

$$\varphi_t(p) = \frac{\partial \ln \theta_t}{\partial \ln p} = \frac{\partial \ln a}{\partial \ln p} = \frac{m}{1 + (\bar{K}p)^n} \tag{38}$$

The function $\varphi_t(p)$ tends asymptotically to m when p tends to zero:

$$\lim_{p \to 0} \varphi_t(p) = m \tag{39}$$

The parameters n and $\bar{K}$ may be calculated by means of the function $\psi_m(p)$ [cf., Eq. (17)]. Moreover, the constant $\bar{K}$ may be evaluated by utilizing the following condition:

$$\varphi_t(p) = \frac{1}{2} m \quad \text{for} \quad \bar{K}p = 1 \tag{40}$$

The parameter a_0 (and also $\bar{K}$) may be evaluated by plotting the following linear relationship:

$$a^{n/m} = a_0^{n/m} - (\bar{K})^{-n} \left(\frac{a^{n/m}}{p^n} \right) \tag{41}$$

After evaluation of the parameters m and n by means of Eqs. (37) and (17), respectively, the parameters $\bar{K}$ and a_0 may be determined by means of the linear relationship given by Eq. (41).

Fig. 5 shows characteristic functions corresponding to the model adsorption isotherm $\ln a$ vs. $\ln p$ (the solid line in the part A of the figure) calculated according to Eq. (21) for $a_0 = 1$, $\bar{K} = 1$, $m = 0.8$ and $n = 0.5$. The function $\varphi_t(p)$ (the dashed line) tends to the asymptotes $\varphi_t = m = 0.8$ at $p \to 0$ and $\varphi_t = 0$ at $p \to \infty$. However, the asymptotes $\ln a = (m \cdot \ln \bar{K} + \ln a_0) + m \cdot \ln p$ (the dotted line) and $\ln a = \ln a_0$ intersect at the point $\ln p = -\ln \bar{K}$ ($\bar{K}p = 1$). The part B of the Fig. 5 shows the functions $\psi_1(p)$ and $\psi_m(p)$ corresponding to the adsorption isotherm plotted in the part A.

The above discussed relatonships are very useful in evaluation of the parameters m, n, $\bar{K}$ and a_0 from experimental adsorption isotherms. Using these relationships the adsorption parameters may be evaluated even graphically.

The interpretation of the adsorption systems by means of Eq. (21) and application of this equation for determining the energy distribution will be presented in the following paper.

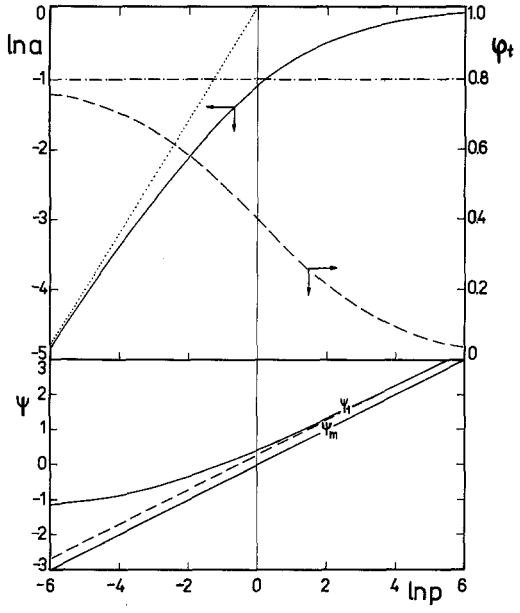

Fig. 5. A) Theoretical adsorption isotherm calculated according to Eq. (21) for $a_0 = 1$, $\bar{K} = 1$, $m = 0.8$ and $n = 0.5$ shown in the plot $\ln a$ vs. $\ln p$ (the solid line) with its asymptote (the dotted line) and corresponding function $\varphi_t(p)$ (the dashed line) with its upper asymptote (the dashed-dotted line). B) Dependences ψ_m and ψ_1 vs. $\ln p$ calculated for the above theoretical isotherm (the solid lines) and the asymptote of ψ_1 (the dashed line)

Appendix

At the limiting pressures $p \to 0$ and $p \to \infty$ the thermodynamically consistent overall adsorption isotherms should satisfy the same conditions as the *Langmuir* equation [cf., Eqs. (10) and (11)]:

$$\lim_{p \to 0} \varphi_t(p) = 1 \tag{A 1}$$

$$\lim_{p \to \infty} \varphi_t^*(p) = -1 \tag{A 2}$$

The conditions (A 1) and (A 2) are fully fulfilled for the overall adsorption isotherms, which produce the energy distribution functions showing the minimum and maximum adsorption energies. Then, these isotherms show correct behaviour at low and high equilibrium pressures, e.g., at low pressures *Henry* behaviour is observed. On the other hand, the analytical integration [Eqs. (1) and (2)] for energy distributions

showing minimum and maximum adsorption energies is frequently very difficult and leads to complex isotherm equations[15,16]. However, our overall adsorption isotherm Eq. (21) produces an energy distribution which tends asymptotically to zero at low and high adsorption energies. The other analytical adsorption isotherms produce also energy distributions showing analogous behaviour at low and high adsorption energies. Only the classical *Freundlich* and *Dubinin-Radushkevich* equations produce energy distributions having minimum adsorption energies, nevertheless they do not fulfil the conditions (A 1) and (A 2). Therefore, these isotherms have only an approximate explanation on the basis of the integral equation (1) with the local *Langmuir* isotherm.

Nevertheless, the real energy distribution, showing minimum and maximum adsorption energies, may be well approximated by the energy distribution showing asymptotical behaviour at low and high adsorption energies. The small deviations between the real and approximating energy distributions appear at low and high adsorption energies, which correspond to high and low equilibrium pressures.

The most popular overall isotherm equations (see Table 2) and the new isotherm Eq. (21) correspond to the energy distributions showing asymptotical behaviour at low and high adsorption energies. The main advantage of these equations is their mathematical simplicity and usefulness to describe experimental data. Although these isotherms do not predict a correct physical behaviour at low equilibrium pressures, they give a good representation of the experimental data in a wide pressure region.

The overall adsorption isotherms, giving non-correct behaviour at low pressure region [the conditions (A 1) and (A 2) are not fulfilled] may be modified so that the conditions (A 1) and (A 2) could be satisfied. We will propose a modification of these overall isotherms improving their behaviour at low pressure region, which is important from the thermodynamical point of view. The idea of this modification was proposed by *Radke* and *Prausnitz*[17]; they modified the classical *Freundlich* equation and obtained the new isotherm Eq. (23) fulfilling the *Henry* law. According to their conception an adsorption isotherm $\theta_t(p)$, satisfying the *Henry* law at low pressures, may be presented as follows:

$$1/\theta_t(p) = 1/(K_H p) + 1/\theta_t^a(p) \tag{A 3}$$

where K_H is the *Henry* constant connected with the maximum adsorption energy and $\theta_t^a(p)$ is the isotherm equation obtained for an energy distribution showing asymptotical behaviour at high adsorption energies, e.g., Eq. (21) and its special cases. For higher pressures the term

$(K_H p)^{-1}$ may be neglected in comparison to $1/\theta_t^a(p)$ and the real adsorption isotherm is well approximated by $\theta_t^a(p)$, i.e., $\theta_t(p) \cong \theta_t^a(p)$. However, at low pressures the isotherm (A 3) fulfills the *Henry* law. Eq. (A 3) may be presented in an equivalent form:

$$\theta_t(p) = \frac{K_H p}{1 + K_H p/\theta_t^a(p)} \tag{A 4}$$

At low pressures $\theta_t^a(p)$ becomes usually the classical *Freundlich* isotherm and the term $K_H p/\theta_t^a(p)$ is small in comparison to unity and it may be neglected. Then, Eq. (A 4) becomes *Henry*'s law. Of course, the energy distribution corresponding to the overall isotherm (A 3) shows the maximum adsorption energy, which determines the *Henry* constant. The modified isotherm Eq. (21) may be written as follows:

$$1/\theta_t(p) = 1/(K_H p) + \left[\frac{1 + (\bar{K}p)^n}{(\bar{K}p)^n}\right]^{m/n} \tag{A 5}$$

This isotherm fulfills *Henry*'s law, however, at higher pressures it becomes Eq. (21).

At the end, we will discuss the *Tóth* isotherm [Eq. (21) with $m = 1$]. Although the *Tóth* isotherm produces an energy distribution function showing asymptotical behaviour at low and high adsorption energies, it predicts *Henry* behaviour at low pressures. This property of the *Tóth* isotherm is caused by a special behaviour of the energy distribution, which rapidly decreases to zero at high adsorption energies and in this way the maximum adsorption energy is defined in a good approximation.

References

[1] *Sips R.*, J. Chem. Phys. **16**, 420 (1948).
[2] *Sips R.*, J. Chem. Phys. **18**, 1024 (1950).
[3] *Misra D. N.*, J. Chem. Phys. **52**, 5499 (1970).
[4] *Misra D. N.*, Surface Sci. **18**, 367 (1969).
[5] *Tóth J., Rudziński W., Waksmundzki A., Jaroniec M., Sokołowski S.*, Acta Chim. Acad. Sci. Hung. **82**, 11 (1974).
[6] *Jaroniec M.*, Surface Sci. **50**, 553 (1975).
[7] *Jaroniec M.*, Advances in Colloid and Interface Sci. **18**, 149 (1983).
[8] *Cerofolini G. F.*, Thin Solid Films **23**, 129 (1974).
[9] *Cerofolini G. F.*, Specialist Periodical Reports "Colloid Science" (*Everett D. H.*, ed.), chap. 2. London: The Chemical Soc.
[10] *Ozawa S., Kusumi S., Ogino Y.*, J. Colloid Interface Sci. **56**, 83 (1976).
[11] *Marczewski A. W., Jaroniec M.*, Monatsh. Chem. **114**, 711 (1983).

[12] *Tóth J.*, Acta Chim. Acad. Sci. Hung. **69**, 311 (1971).
[13] *Tóth J.*, Proceedings Int. Conf. "Colloid and Surface Sci." (*Wolfram E.*, ed.), p. 41. Budapest: Akademiai Kiado. 1975.
[14] *Dąbrowski A., Jaroniec M.*, J. Colloid Interface Sci. **73**, 475 (1980).
[15] *Rudnitsky L. A., Alexeyev A. M.*, J. Catalysis **37**, 232 (1975).
[16] *Bräuer P., Heller G.*, Wiss. ZFS Univ., Jena, Math.-Naturwiss. R. **26**, 719 (1977).
[17] *Radke C. J., Prausnitz J. M.*, Ind. Eng. Chem. Fund. **11**, 445 (1972).